Bariza BOUKNI[1] iD
Sara BENSALEM[1] iD
Mohamed Lyes Kamel KHOUADJIA[1] iD
Oussama TEMAMI[1] iD
Salim HAMLAOUI[1]
Cherif BELEBCHOUCHE[1,2]✉ iD

[1] University Frères Mentouri Constantine 1, Department of Civil Engineering, Laboratory of Materials and Durability of Constructions, Algeria
[2] Setif 1 University – Ferhat Abbas, Faculty of Technology, Department of Civil Engineering, Algeria

The influence of iron powder content on the fresh and hardened properties of mortar

Introduction

Concrete, a cornerstone of construction, typically combines cement, sand, gravel, and water. Researchers have explored incorporating waste materials to enhance their properties or eco-friendliness (Krikar et al., 2018; Largeau et al., 2018). Waste materials, often discarded as useless or obsolete (Harrison, Ed., 2023), can provide multiple advantages when incorporated into concrete. Utilizing

✉ cherif.belebchouche@univ-setif.dz

these materials can reduce waste disposal, decrease the demand for traditional raw materials, and create more sustainable building solutions (Miah et al., 2021). Recent research has highlighted the potential benefits of integrating waste materials into mortar and concrete mixtures. Recycled construction and demolition waste, such as bricks and road debris, has been examined as a viable and economical alternative to traditional aggregates and cement, thereby reducing environmental impact (Belebchouche et al., 2024). Moreover, waste paper and plastic waste have been successfully utilized to improve the mechanical properties of mortars, particularly in applications like wall plastering (Harabi et al., 2024). Incorporating steel and aluminum fibers has been shown to enhance the strength and durability of concrete, mitigating the propagation of cracks and microcracks (Khouadjia et al., 2023). Finally, the addition of glass waste has been observed to positively influence mortars' compressive and flexural strength (Małek et al., 2021).

The global metal powder industry generates over 700,000 tons of iron-based waste annually, presenting a substantial opportunity for valorization in sustainable construction materials (Khouadjia et al., 2025). Among these underutilized industrial by-products, waste iron powder (IP) resembles fine cement in particle size and characteristics, making it a promising candidate for partial replacement in mortars and concrete (Giovanni et al., 2024). Instead of discarding this waste, which contributes to metal loss and environmental pollution, its inherent mechanical properties can be leveraged for construction applications, promoting ecological sustainability (Thakur et al., 2019; Fahad & Jassim, 2020).

Numerous studies have explored the potential of incorporating IP waste as a substitute for either cement or aggregates. For instance, research has shown that including waste materials can lead to significant benefits. In a relevant study, incorporating 20% waste industrial tire powder (WITP) into mortar mixtures resulted in a 20% reduction in cement consumption and a corresponding 19.98% decrease in overall economic cost (Cui et al., 2022). This demonstrates the broader economic and environmental advantages of using industrial construction by-products.

Other studies have investigated the use of recycled IP as a partial replacement for sand and cement. These studies have yielded mixed results. While some research (Largeau et al., 2018; Cui et al., 2022) observed a decrease in flowability and an increase in dry density with increasing IP content. Researchers Fahad and Jassim (2019), Lu et al. (2020), Miah et al. (2020), and Miah et al. (2021) reported improvements in dry density, porosity, and water absorption. Research conducted by Largeau et al. (2018) revealed that partial substitution of portland cement with industrial by-products (IP) at varying levels (1.5%, 2.5%, 3.5%,

and 5% by weight) resulted in a decline in workability and a substantial decrease in porosity. Notably, 21.88% and 26.77% porosity reductions were observed at replacement levels of 1.5% and 2.5%, respectively. Furthermore, Dias et al. (2020) observed a more homogeneous behavior in mixtures incorporating IP and concerning the effect of IP on mechanical properties. Largeau et al. (2018) reported improved compressive and tensile strengths of concrete with up to 5% iron powder replacement, with optimal values observed at 2.5% and 1.5%, respectively. Similarly, Lu et al. (2020) found that the incorporation of iron powder led to an increase in tensile bond strength, compressive strength, and flexural strength. Furthermore, Miah et al. (2021) investigated the use of waste iron powder (WIP) as a partial replacement for fine aggregates, observing significant enhancements in the compressive, tensile, and flexural strengths of mortar up to a 7.5% replacement level. These findings align with Dias et al. (2020) and Kong et al. (2023), who reported increases in 28-day compressive strength of up to 13.2% and improvements in both axial compression and tensile strength of 13.83% and 14.34%, respectively, when IP was incorporated into concrete. However, other research has found that recycling iron powder (IP) decreased compressive strength significantly with increasing IP percentage, particularly at higher curing ages (Tayeh & Al Saffar, 2018; Giovanni et al., 2024). The results indicated a general trend of reduced compressive strength with increasing iron powder content compared to control concrete (Belebchouche et al., 2024). The optimal replacement percentage was determined to be 12%, which yielded the highest compressive and flexural strength in the shortest curing time. Increasing the iron waste content beyond 12% led to a decrease in concrete strength (Krikar et al., 2018). Studies have shown that the addition of IP can enhance certain aspects of concrete performance. For instance, the nucleation and pozzolanic effects of waste iron powder (WIP) have been observed. It has been observed that WIP promotes cement hydration, leading to improved durability (Cui et al., 2022). However, concerns have also been raised regarding dimensional stability, with shrinkage and expansion observed in mortars containing IP, particularly at higher replacement percentages (exceeding 5%) (Miah et al., 2020). Furthermore, research suggests that IP can act as a barrier, hindering the access of chloride ions to steel reinforcement, thereby mitigating the risk of corrosion (Largeau, 2018; Largeau et al., 2018). This research investigates the potential of IP as a viable alternative to cement in mortar formulations. The study primarily focuses on evaluating the influence of IP incorporation on both the fresh and hardened state properties of mortar. In the fresh state, this encompasses an assessment of flow time, consistency, setting time, air content, and density, while hardened state properties under investigation

include compressive and flexural strengths. This research offers significant practical implications by providing a viable and sustainable pathway for utilizing industrial waste, reducing landfill burden, conserving natural resources, and developing greener, high-performance construction materials, thereby contributing valuable insights into the feasibility and substantial benefits of incorporating iron powder as a sustainable construction material.

Materials

Cement components

Cement. This study employed commercial portland cement (CEM I) with a 42.5 MPa strength class, sourced from the SPA Biskra cement factory. The cement's quality adheres to the requirements of standard NF EN 197-1 (AFNOR, 2012a). The chemical and mineralogical compositions of the cement are presented in Table 1. The potential mineralogical composition was subsequently calculated using the empirical formula of Bogue (1947).

TABLE 1. Chemical and physical characteristics of portland cement CEM I/42.5R

Specification	Chemical composition							
Content [%]	SiO_2	Al_2O_3	Fe_2O_3	CaO	MgO	K_2O	TiO_2	Na_2O
	20.14	5.53	3.54	61.60	0.19	0.03	0.008	0.06
	Mineralogical composition							
Content [%]	C_3S		C_2S		C_3A		C_4AF	
	55.43		15.53		8.67		10.76	
	Physical properties							
Specific density [$kg \cdot m^{-3}$]	3 100.0							
Fineness [$cm^2 \cdot g^{-1}$]	3 500.0							
Initial setting time [min]	170.0							
Final setting time [min]	255.0							

Source: own work.

Water. The tap water used in this study was obtained from the Genie Civil Laboratory at the University of Constantine 1. The water temperature was maintained at 20 ±2°C. Water quality met the requirements of the NF EN 206+A2/CN standard (Association Française de Normalisation [AFNOR], 2022a).

Sand. Crushed sand (0/5 mm) obtained from the National Company of Aggregates in Constantine was used in this study. Table 2 presents

the chemical and physical properties of the crushed sand. All physical property measurements adhered to the following standards: NF EN 933-1 (AFNOR, 2012c), NF EN 933-8+A1 (AFNOR, 2015), and NF EN 1097-7 (AFNOR, 2022b). Figure 1 illustrates the grading curves of the different sands.

TABLE 2. Chemical properties of crushed sands

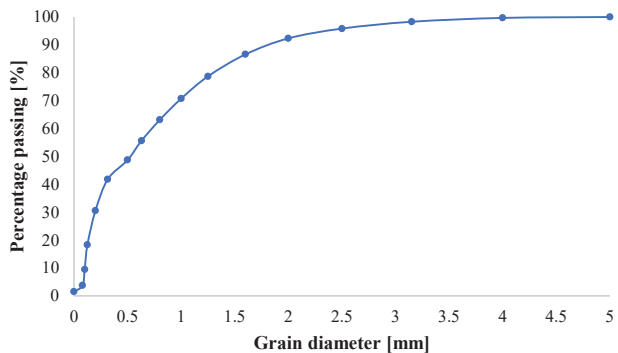| Specification	Chemical composition							
Content [%]	SiO_2	Al_2O_3	Fe_2O_3	CaO	MgO	K_2O	TiO_2	Na_2O
	0.05	0.03	0.02	56.03	0.19	0.03	0.008	0.06
	Physical properties							
Specific density [kg·m^{-3}]	2,750.0							
Apparent density [kg·m^{-3}]	1,460.0							
Fineness [cm^2·g^{-1}]	3,700.0							
Sand equivalent [%]	69.0							
Absorption coefficient [%]	1.1							

Source: own work.

FIGURE 1. Grading curves of crushed sand

Source: own work.

Iron powder. This material was procured from Algerian Qatari Steel (AQS). This IP largely originates from industrial by-products, notably fine dust from iron and steel machining and fabrication, as well as sludges from furnaces and air pollution control systems. We employed scanning electron microscopy (SEM) for morphological analysis, energy dispersive X-ray spectroscopy (EDS) for elemental composition, and X-ray diffraction (XRD) for phase identification and crystallinity. As previously documented in NF EN 1097-7 (AFNOR, 2022b), EDS analysis (Fig. 2) of the IP confirmed a high iron content, along with trace elements such as O, Ca, Si, Mg, Na, Al, K, and S. On the other hand, the XRD pattern (Fig. 3) identified iron

oxides, specifically Fe_2O_3 and FeO. Although some iron-rich materials can exhibit pozzolanic activity, the absence of crystalline silica or alumina phases in the pattern suggests limited pozzolanic reactivity in this material. The iron particles, observed in Figure 4, display irregular shapes and some agglomeration. This structure can impact air entrainment, water absorption, and compressive strength.

TABLE 3. Chemical and physical properties of iron powder

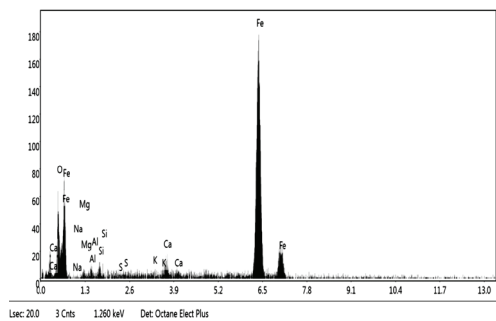| Specification	Chemical properties							
Content [%]	SiO_2	Al_2O_3	Fe_2O_3	CaO	MgO	K_2O	FeO	P_2O_5
	4.80	1.13	64.75	0.85	0.07	–	1.00	0.05
	Physical properties							
Specific density [kg·m^{-3}]	2,250.0							
Apparent density [kg·m^{-3}]	1,220.0							

Source: own work.

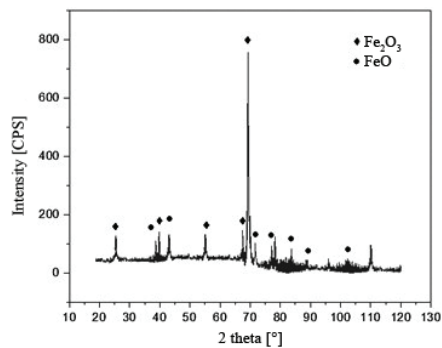FIGURE 2. EDS spectrum of iron powder
Source: own work.

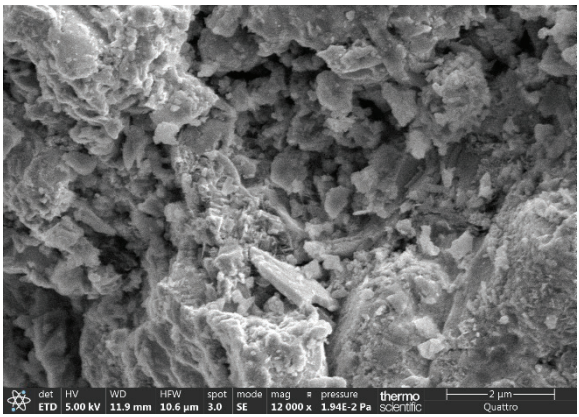FIGURE 3. XRD patterns of iron powder
Source: own work.

FIGURE 4. SEM image of iron powder

Source: own work.

Mix proportions

A reference mortar mixture was prepared, comprising 75% sand and 25% cement with a water-to-cement (W/C) ratio of 0.5. To systematically assess the effects of iron powder on mortar properties, the sand content of the reference mixture was progressively replaced with varying percentages of iron powder. Six distinct iron powder replacement levels were investigated: 1%, 2%, 3%, 4%, 10%, and 20%. This systematic replacement resulted in eight distinct mortar mixtures in total, including the control mixture. The detailed quantitative compositions of all eight mixtures, including the exact proportions of cement, sand, water, and iron powder for each mix, are presented in Table 4.

TABLE 4. Compositions of mortars

Designation	Crushed sand content [g]	Cement content [g]	Iron powder content [g]	Water content [g]
MC0	1 350.0	450.0	0	225.0
MIP1	1 350.0	445.5	4.5	225.0
MIP2	1 350.0	441.0	9.0	225.0
MIP3	1 350.0	436.5	13.5	225.0
MIP4	1 350.0	432.0	18.0	225.0
MIP5	1 350.0	427.5	22.5	225.0
MIP10	1 350.0	405.0	45.0	225.0
MIP20	1 350.0	360.0	90.0	225.0

Source: own work.

All mortar mixtures were prepared in accordance with the specifications outlined in EN206+A2/CN (AFNOR, 2022a). This involved using a standard laboratory planetary mixer and following a specific mixing sequence: dry components were mixed for 2 mins, water was added over 30 s, followed by 2 mins of mixing at high speed. To ensure statistical robustness and reproducibility of results, all experimental tests for each mortar mixture were repeated a minimum of three times. The reported results represent the average of these replicates, with standard deviations provided where appropriate.

After preparation, the fresh mortar mixtures were cast into prismatic molds with dimensions of $4 \times 4 \times 16$ cm for subsequent evaluation of flexural strength and compressive strength. The molds were filled in two layers, with each layer compacted using a vibratory table for 60 s. Following casting, the samples were cured in their molds at 20 ±2°C and over 95% relative humidity for a period of 24 h. After this initial curing period, the samples were carefully demolded and subsequently left to cure in ambient air conditioning at 20 ±2°C for 28 days until testing.

Results and discussion

Setting time and consistency

The setting time and consistency of the mortar were determined using a Vicat apparatus following EN 196-3 (European Committee for Standardization [CEN] 2016). For consistency, the mortar was placed in a conical mold, and the 10 mm plunger penetration depth was measured, aiming for a standard value. For setting times, a specific needle was used to track penetration; initial setting was when the needle no longer reached the bottom, and final setting was when only a surface impression remained. These tests were conducted at regular intervals until both points were identified. Figures 5 and 6 present the results.

Figure 5 presents the setting times of mortars with varying iron powder content. The control mortar (MC) without iron powder exhibits a setting time of approximately 2 h. The mortars with 1% (MIP1) and 2% (MIP2) iron powder show a slight increase in setting time compared to the control. However, a substantial increase in setting time was observed for MIP3, MIP4, and MIP5, reaching a maximum of 3 h. Interestingly, as the iron powder content increases to 10% (MIP10) and 20% (MIP20), the setting time decreases, falling back to approximately 2 h. The initial addition of small amounts of iron powder (MIP1,

MIP2) to the cement paste resulted in a slight increase in setting time. This can be attributed to the nucleation effect of the iron particles, which act as nucleation sites for the formation of hydration products, initially accelerating the setting process. However, as the iron powder content increased further (MIP3, MIP4, MIP5), the setting time began to delay significantly. The mixture likely required more water to achieve the desired workability. This is probably because numerous nucleation sites cause rapid water consumption. This observation aligns with previous research (Thakur et al., 2019).
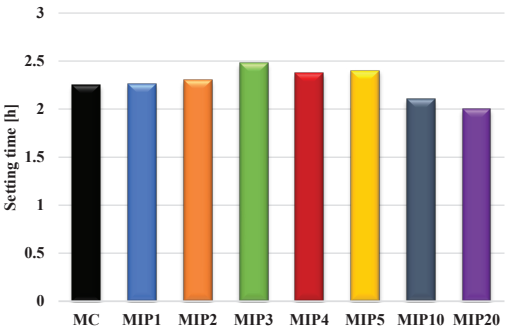

FIGURE 5. Evolution of setting time according to the substitution rate of iron powder
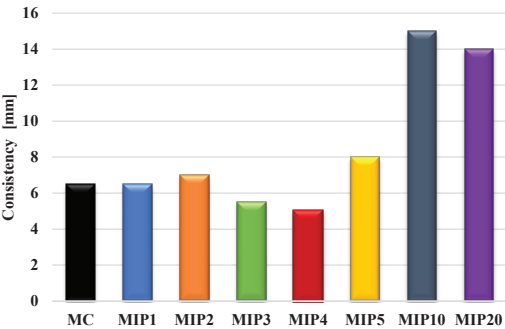Source: own work.

FIGURE 6. Evolution of consistency according to the substitution rate of iron powder
Source: own work.

Conversely, at higher iron powder concentrations (MIP10, MIP20), the setting time decreased. This could be attributed to several factors. Firstly, the excessive amount of iron powder may have interfered with the hydration process, potentially hindering the proper packing of cement particles and reducing the overall

reaction rate. Secondly, the presence of a large number of iron particles may have disrupted the formation of the hydration product network, leading to a faster setting time.

Concerning the evolution of consistency as a function of the iron powder substitution rate, as shown in Figure 6, the results indicate that the MC exhibits a consistency of 6 mm. Upon introducing 1–5% iron powder (MIP1 to MIP5), the consistency shows minor fluctuations, suggesting a limited impact at these low concentrations. These results agree with those of Largeau et al. (2018).

However, a significant increase in consistency is observed in higher iron powder contents (MIP10 and MIP20), reaching 15 mm and 14 mm, respectively. This trend likely arises from the increased particle size and surface area of the iron powder, leading to greater interparticle friction and a stiffer mortar mix.

Air content and bulk density

To characterize the fresh mortar properties, air content was determined using a mortar aerometer in accordance with EN 1015-7 (AFNOR, 1999). This involved filling a standardized vessel with fresh mortar, striking off the excess, and then using the aerometer to measure the entrapped air volume based on the pressure method. Furthermore, the bulk density of the fresh mortar was measured following NF EN 1015-6/A1 (AFNOR, 2007). For this, a known volume of fresh mortar was carefully placed into a tared container of specified dimensions, and its mass was determined. The bulk density was then calculated by dividing the mass of the mortar by the volume of the container. The resulting air content and bulk density values for each mortar mixture are presented in Figures 7 and 8, respectively.
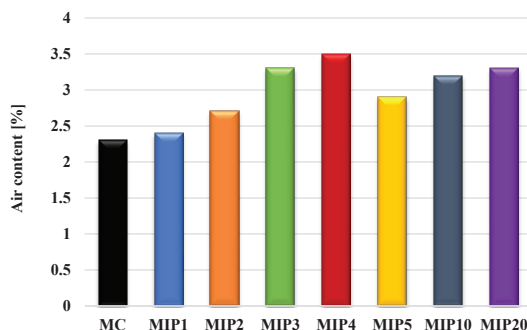

FIGURE 7. Evolution of air content according to the substitution rate of iron powder
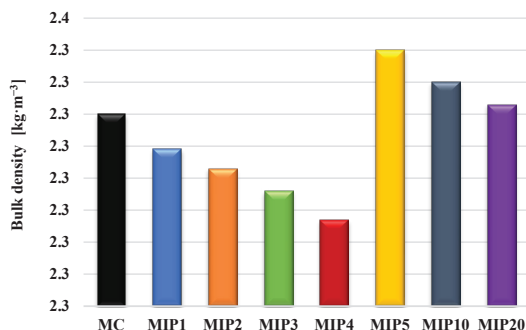Source: own work.

FIGURE 8. Evolution of bulk density according to the substitution rate of iron powder

Source: own work.

Figure 7 depicts the air content of mortars expressed as a percentage. The MC, devoid of iron powder, displays an air content of approximately 2%. The inclusion of 1% (MIP1) and 2% (MIP2) iron powder results in a modest increase in air content. However, a slight rise in air content is observed for MIP3 (3% iron powder), MIP4 (4% iron powder), and MIP5 (5% iron powder), with air content increasing up to 3.5%. The observed initial increase in air content with the addition of small amounts of iron powder (MIP1, MIP2) can be attributed to the increased surface roughness and irregular shapes of the iron particles, as shown in Figure 4. These characteristics contribute to enhanced air entrainment within the mortar matrix. The iron particles, acting as nucleation sites, likely trap air bubbles during mixing. This effect becomes more pronounced for MIP3 and MIP4, leading to substantial increases in the measured air content. Specifically, MIP3 demonstrated a 43.47% increase, while MIP4 exhibited a 52.17% increase. An intriguing observation was the decreased air content in mortars with higher iron powder concentrations (MIP10, MIP20) compared to MIP4. This phenomenon may be attributed to several factors. Firstly, at elevated iron powder concentrations, particle agglomeration might occur, reducing the overall surface area available for air bubble nucleation. Secondly, the increased viscosity of the mortar mix at higher iron powder contents, as previously observed in consistency tests, could impede the movement and dispersion of air bubbles within the matrix, consequently limiting air entrainment. These results are concordant with the findings of work by Khouadjia et al. (2025). The results shown in Figure 8 concerning the evolution of bulk density as a function of the substitution rate of iron powder indicate that the addition of iron powder from 1% to 4% leads to a decrease in bulk density (up to 1.42%

for MIP4). However, as the iron powder content increases to 5% (MIP5), 10% (MIP10), and 20% (MIP20), the bulk density significantly increases, reaching values of 2.34 kg·m^{-3}, 2.33 kg·m^{-3}, and 2.323 kg·m^{-3}, respectively, compared to the control concrete, which has a density of 2.32 kg·m^{-3}. The initial reduction in bulk density observed with the addition of small amounts of iron powder (MIP1, MIP2, MIP3, MIP4) can be attributed to increased porosity within the mortar matrix. Iron particles possessing a higher density than the constituent cement and sand can disrupt the natural particle packing arrangement. This disruption results in the formation of voids and consequently a decrease in the overall bulk density of the mortar mixture.

On the other hand, the increase in bulk density observed at higher iron powder concentrations (MIP5, MIP10, MIP20) strongly suggests a modification of the mortar's microstructure. This enhancement is likely due to a combination of factors. Firstly, the increased presence of iron particles likely improves particle packing within the mortar matrix, reducing voids and leading to a more compact structure. Secondly, the intrinsic high density of iron significantly contributes to the overall mass of the mortar, directly resulting in an increase in bulk density. These results are similar to those obtained by Khouadjia et al. (2025) concerning the use of iron powder.

Workability (flow time)

The flow time of all mortar mixtures was determined using the LCPC workability meter (French test), in accordance with the standard NF P 18-452 (AFNOR, 2017a). The results of the flow time test are presented in Figure 9.
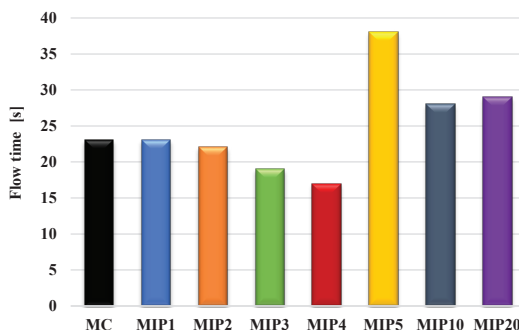

FIGURE 9. Evolution of flow time according to the substitution rate of iron powder
Source: own work.

Figure 9 shows that the MC exhibited a flow time of 23 s. The incorporation of 1–2% iron powder (MIP1 to MIP2) had a minimal impact on flow time, with values remaining largely consistent with the MC. However, a notable decrease in flow time is observed for MIP3 and MIP4, suggesting a reduction in viscosity and an increase in workability at these intermediate concentrations. This enhanced flowability can be attributed to several factors. Firstly, the incorporation of iron powder likely improved particle dispersion within the mortar matrix. Acting as fillers, the iron particles may have facilitated denser packing of cement particles, minimized voids, and promoted smoother flow. Secondly, interactions between the iron powder and cement particles may have altered the surface properties of the cement, potentially reducing particle agglomeration. This surface modification could have contributed to a more fluid and workable mortar. These results are consistent with previous findings (Ruidong et al., 2021).

However, at higher iron powder contents (MIP5, MIP10, and MIP20), a significant increase in flow time is observed, reaching 38 s, 28 s, and 29 s, respectively. This increase in flow time indicates that higher concentrations of iron powder can adversely affect the workability of the mortar. Several factors contribute to these results. A higher concentration of iron powder concentration likely leads to particle agglomeration, forming larger clusters within the mortar that impede flow and increase viscosity. Additionally, the iron powder may absorb some of the mixing water, reducing the available water and making the mortar stiffer and less workable. Consequently, this results in longer flow times, negatively impacting workability and application. These observations are consistent with findings by Bogue (1947) and Han et al. (2022).

Furthermore, the increased density of the mortar (Fig. 8), due to the addition of high concentrations of iron powder, can also contribute to the observed decrease in workability. A denser mortar may exhibit greater resistance to flow and deformation, leading to increased difficulty in shaping and placing the material.

Compressive strength

Compressive strength tests were performed on mortar specimens at 28 days of curing. We followed the NF EN 12390-3 standard (AFNOR, 2012b) precisely, using a universal testing machine to apply a controlled compressive load until failure. For each mix, six replicate specimens were tested to ensure reliability. The reported values in Figure 10 represent the average compressive strength obtained from these three measurements, providing a robust and representative data point.
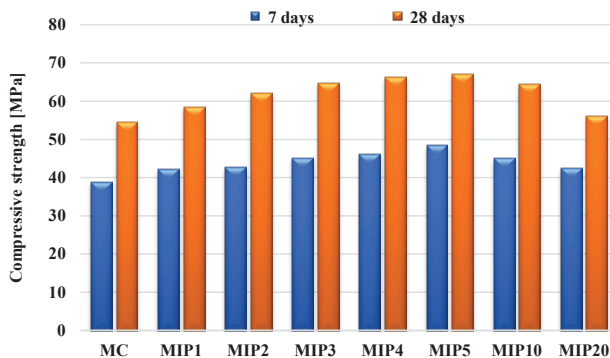
FIGURE 10. Evolution of compressive strength according to the substitution rate of iron powder
Source: own work.

Figure 10 illustrates the compressive strength of mortars at 7 days and 28 days, comparing a MC with mortars containing varying amounts of iron powder (MIP1 to MIP20). Overall, the presence of iron powder generally enhances the compressive strength, particularly at 28 days. While the 7-day strength shows a slight increase of approximately 10–12.5% compared to the control, the 28-day strength demonstrates a more substantial improvement (8–18%), suggesting that iron powder promotes strength development over time. The highest compressive strength was achieved for mortars containing 5% iron powder, exceeding 67.11 MPa. These results align with the observed trends in air content and bulk density. Specifically, the air content of the 5% iron powder mixture (MIP 5) increased slightly, while the bulk density remained relatively high. This improvement in strength can be attributed to several mechanisms: the iron powder acts as a filler material, enhances particle packing density, and facilitates better mechanical interlocking within the mortar matrix. As a result, this denser matrix leads to a more compact and robust structure. The presence of iron powder may influence the formation of ettringite, a sulfate-bearing compound that contributes to strength development over time (Tao & Dang, 2016; Largeau et al., 2018; Cui et al., 2024). Incorporating iron powder into concrete at levels of 10% and 20% resulted in reduced compressive strength at both 7 days and 28 days. This weakening effect is likely due to the iron powder replacing cement, which consequently impedes the formation of calcium silicate hydrate (C-S-H) – a key component for concrete strength, particularly in the initial stages (Giovanni et al., 2024).

Three-point flexural strength

The three-point flexural strength of the specimens was determined according to the European standard NF EN 12390-1 (AFNOR, 2017b). Each specimen was centrally loaded at a controlled rate while being supported at two points. The maximum load at failure was recorded, and the flexural strength was calculated using the specified formula, considering the specimen's dimensions. These tests provided crucial data on the material's resistance to bending. The results are presented in Figure 11.
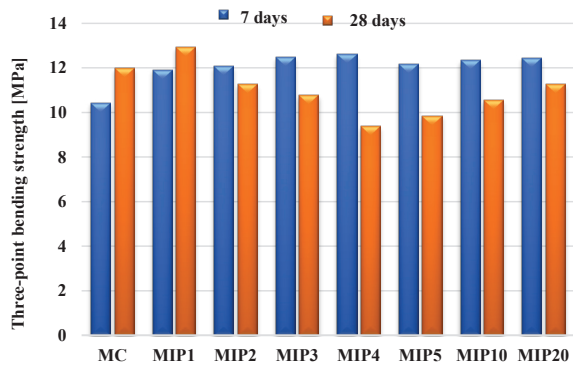

FIGURE 11. Evolution of three-point bending strength according to substitution rate of tuff with iron powder
Source: own work.

Figure 11 illustrates the three-point bending strength of mortars containing varying amounts of iron powder at 7 days and 28 days. The MC exhibits a bending strength of approximately 10 MPa at 7 days and 12 MPa at 28 days. The addition of iron powder initially leads to an increase in strength at 7 days, with MIP2 showing the highest increase of 30% compared to the control. This early strength gain can be attributed to the nucleation and refinement of cement hydration products due to the presence of iron powder.

However, in 28 days, the situation changes. While some mortars with iron powder (MIP5, MIP10) show a slight increase in strength (8.33% and 4.17%, respectively), others (MIP2, MIP3, MIP4, and MIP20) exhibit a significant decrease in strength compared to the MC, with MIP4 showing the largest decrease of 25%. This suggests that at higher iron powder concentrations, mechanisms such as iron powder aggregation or interference with the normal hydration process of cement might be detrimental to the long-term strength development of the mortar (Largeau et al., 2018; Giovanni et al., 2024).

These findings highlight the complex influence of iron powder on the mechanical behavior of mortars. While it can enhance early strength, its effect on long-term strength is more nuanced and requires careful optimization of the iron powder content to prevent negative impacts on three-point bending.

Conclusions

This study investigates the feasibility of using waste iron powder (IP) as a partial replacement for cement in mortar, with the goal of developing sustainable construction materials from industrial by-products. Our research specifically evaluates the effects of different IP percentages (1–20% by weight of cement) on the fresh and hardened properties of mortar. This work offers a viable pathway for utilizing industrial waste and contributes to reducing environmental impact.

The incorporation of iron powder significantly influenced various mortar properties. A complex relationship was observed between IP content and setting time, where small additions (1–2%) slightly delayed setting, while higher concentrations (beyond 5%) progressively accelerated it. Consistency remained relatively stable at low IP concentrations (1–5%) but significantly decreased at higher levels (10–20%), likely due to the increased surface area of IP leading to a higher water demand.

Air entrainment varied with IP content; small additions (1–2%) modestly increased air content, higher concentrations (3–4%) significantly increased it, and even higher concentrations (10–20%) led to a decrease. Mortar flow time was minimally affected at low IP concentrations (1–4%) but significantly increased at higher levels (5%, 10%, 20%), attributed to factors such as particle agglomeration, increased interparticle friction, and potentially higher water absorption by the IP.

Crucially, incorporating iron powder significantly improved compressive strength, particularly at 28 days. Mortar, with 5% IP (MIP5), achieved the highest 28-day compressive strength of 67.11 MPa, representing a notable enhancement attributed to improved particle packing and increased density. While initial flexural strength showed promise (30% increase for MIP2 at 7 days), this benefit diminished over time, with higher IP concentrations leading to significant reductions in 28-day flexural strength (MIP4 showing a 25% decrease compared to the control).

Based on these comprehensive findings, a 5% waste iron powder replacement (WIP5) stands out as the optimal percentage, consistently demonstrating superior performance in terms of compressive strength and overall balanced properties – a conclusion directly supported by our results.

These findings collectively emphasize the importance of carefully optimizing iron powder content to achieve the desired mechanical properties while balancing various characteristics of the mortar. This research offers specific insights into how iron powder affects mortar performance, guiding future applications and material design. Future research should focus on exploring hybrid binder systems with other materials that could mitigate issues like reduced flexural strength. Crucially, durability studies (e.g., sulfate and chloride resistance) and life cycle assessments are vital to confirm the long-term viability and environmental benefits of these sustainable mortars in practical applications.

References

Association Française de Normalisation [AFNOR] (1999). *Méthodes d'essai des mortiers pour maçonnerie. Partie 7: détermination de la teneur en air du mortier frais* (NF EN 1015-7) [*Methods of test for mortar for masonry. Part 7: determination of air content of fresh mortar*]. AFNOR.

Association Française de Normalisation [AFNOR] (2007). *Méthodes d'essai des mortiers pour maçonnerie. Partie 6: détermination de la masse volumique apparente du mortier frais* (NF EN 1015-6/A1) [*Methods of test for mortar for masonry. Part 6: determination of bulk density of fresh mortar*]. AFNOR.

Association Française de Normalisation [AFNOR] (2012a). *Ciment. Partie 1: Compostition, spécifications et critères de conformité des ciments courants* (NF EN 197-1) [*Cement. Part 1: composition, specifications and conformity criteria for common cements*]. AFNOR.

Association Française de Normalisation [AFNOR] (2012b). *Essais pour béton durci. Partie 3: résistance à la compression des éprouvettes* (NF EN 12390-3) [*Tests for hardened concrete. Part 3: compressive strength of the specimens*]. AFNOR.

Association Française de Normalisation [AFNOR] (2012c). *Essais pour déterminer les caractéristiques géométriques des granulats. Partie 1: détermination de la granularité. Analyse granulométrique par tamisage* (NF EN 933-1) [*Tests for geometrical properties of aggregates. Part 1: determination of particle size distribution. Sieving method*]. AFNOR.

Association Française de Normalisation [AFNOR] (2015). *Essais pour déterminer les caractéristiques géométriques des granulats. Partie 8: évaluation des fines. Équivalent de sable* (NF EN 933-8+A1) [*Tests for geometrical properties of aggregates. Part 8: assessment of fines. Sand equivalent test*]. AFNOR.

Association Française de Normalisation [AFNOR] (2017a). *Bétons. Mesure du temps d'écoulement des bétons et des mortiers au maniabilimètre* (NF P 18-452) [*Concretes. Measuring the flow time of concretes and mortars using a workabilitymeter*]. AFNOR.

Association Française de Normalisation [AFNOR] (2017b). *Essais pour béton durci. Partie 1: Forme, dimensions et autres exigences aux éprouvettes et aux moules* (NF EN 12390-1)

[*Testing hardened concrete. Part 1: shape, dimensions and other requirements for specimens and moulds*]. AFNOR.

Association Française de Normalisation [AFNOR] (2022a). *Béton. Spécification, performance, production et conformité. Complément national à la norme* (NF EN 206+A2) [*Concrete. Specification, performance, production and conformity. National addition to the standard*]. AFNOR.

Association Française de Normalisation [AFNOR] (2022b). *Essais pour déterminer les caractéristiques mécaniques et physiques des granulats. Partie 7: détermination de la masse volumique réelle du filler. Méthode au picnomètre* (NF EN 1097-7) [*Tests for mechanical and physical properties of aggregates. Part 7: determination of the particle density of filler. Pyknometer method*]. AFNOR.

Belebchouche, C., Temami, O., Khouadjia, M. L. K., Hamlaoui, S., Berkouche, A., & Chouadra, T. (2024). Recycling of brick and road demolition waste in the production of concrete. *Science, Engineering and Technology*, *4*(2), 14–23. https://doi.org/10.54327/set2024/v4.i2.154

Bogue, R. H. (1947). *Chemistry of Portland cement*. Reinhold.

Cui, L., Chen, P., Wang, L., Xu, Y., & Wang, H. (2022). Reutilizing waste iron tailing powders as filler in mortar to realize cement reduction and strength enhancement. *Materials*, *15*(2), 541. https://doi.org/10.3390/ma15020541

Cui, L., Xu, Y., Wang, L., Ying, P., & Wang, H. (2024). Investigating the hydration characteristics of iron tailings powder cement mortar produced by the mortar substitution method. *Journal of Building Engineering*, *81*, 108100. https://doi.org/10.1016/j.jobe.2023.108100

Dias, R., Bigotto, S., Benjamim, D. U., Chotolli, D. L., & de Souza, M. V. (2020). Concrete mixture with the use of iron powder waste for coarse aggregate doping. *International Journal of Multidisciplinary Sciences and Engineering*, *11*(2), 18–24. https://www.ijmse.org/Volume11/Issue2/paper3_11_2.pdf

European Committee for Standardization [CEN] (2016). *Methods of testing cement. Part 3: Determination of setting times and soundness* (EN 196-3).

Fahad, B. M., & Jassim, K. S. (2020). Behaviour of cement mortar containing iron waste powder as a substitute for sand. *IOP Conference Series: Materials Science and Engineering*, *737*(1), 012064. https://doi.org/10.1088/1757-899X/737/1/012064

Giovanni, D., Rumbyarso, Y. P. A., & Siagian, B. (2024). Analysis of concrete compressive strength with partial substitution of iron powder waste as fine aggregate. *International Journal of Multi Science*, *4*(02), 122–129.

Han, F., Zhang, H., Liu, J., & Song, S. (2022). Influence of iron tailing powder on properties of concrete with fly ash. *Powder Technology*, *398*, 117132. https://doi.org/10.1016/j.powtec.2022.117132

Harabi, H., Khouadjia, M. L. K., Bensalem, S., Isleem, H. F., & Khishe, M. (2024). Effect of waste paper aggregate and polyethylene terephthalate on mortar performance. *Scientific Reports*, *14*(1), 29588. https://doi.org/10.1038/s41598-024-80914-0

Harrison, R. M. (Ed.). (2023). *Pollution: causes, effects, and control*. Royal Society of Chemistry.

Khouadjia, M. L. K., Bensalem, S., Belebchouche, C., Boumaza, A., Hamlaoui, S., & Czarnecki, S. (2025). Sustainable geopolymer tuff composites utilizing iron powder waste: rheological

and mechanical performance evaluation. *Sustainability*, *17*(3), 1240. https://doi.org/10.3390/su17031240

Khouadjia, M. L. K., Bensalem, S., Belkadi, A. A., Kessal, O., & Sebti, M. A. (2023). Influence of the shape and content of steel and aluminum fibers from industrial lathe wastes on the physico-mechanical and rheological behavior of concrete. *Journal of Applied Engineering Sciences*, *13*(26), 207–214. https://doi.org/10.2478/jaes-2023-0026

Kong, L., Xie, S., Wang, C., & Wang, L. (2023). Effect of iron tailings as fine aggregate and mineral admixture on strength and microstructure of cement mortar. *International Journal of Concrete Structures and Materials*, *17*(1), 24. https://doi.org/10.1186/s40069-023-00584-6

Krikar, M., Noori, G., & Ibrahim, H. H. (2018). Mechanical properties of concrete using iron waste as a partial replacement of sand. *Eurasian Journal of Science and Engineering*, *3*(3), 75–82. https://doi.org/10.23918/eajse.v3i3p75

Largeau, M. A. (2018). *Effect of iron powder partially used as Portland cement replacement on the structural properties of concrete* (doctoral dissertation). Jomo Kenyatta University of Agriculture and Technology.

Largeau, M. A., Mutuku, R., & Thuo, J. (2018). Effect of iron powder (Fe_2O_3) on strength, workability, and porosity of the binary blended concrete. *Open Journal of Civil Engineering*, *8*(04), 411. https://doi.org/10.4236/ojce.2018.84029

Lu, Y., Huang, J., & Gao, Y. (2020). Study on the preparation and properties of modified functional mortar mixed with reduced iron powder. *IOP Conference Series: Materials Science and Engineering*, *735*(1), 012018. https://doi.org/10.1088/1757-899X/735/1/012018

Małek, M., Jackowski, M., Łasica, W., Kadela, M., & Wachowski, M. (2021). Mechanical and material properties of mortar reinforced with glass fiber: An experimental study. *Materials*, *14*(3), 698. https://doi.org/10.3390/ma14030698

Miah, M. J., Ali, M. K., Paul, S. C., John Babafemi, A., Kong, S. Y., & Šavija, B. (2020). Effect of recycled iron powder as fine aggregate on the mechanical, durability, and high temperature behavior of mortars. *Materials*, *13*(5), 1168. https://doi.org/10.3390/ma13051168

Miah, M. J., Miah, M. S., Paul, S. C., Kong, S. Y., Babafemi, A. J., Ali, M. K., & Patoary, M. M. H. (2021). Waste iron powder is used as aggregate and as a binder in mortar production. *Magazine of Civil Engineering*, *108*(8), 10810. https://doi.org/10.34910/MCE.108.10

Ruidong, W., Yu, S., Juanhong, L., Linian, C., Guangtian, Z., & Yueyue, Z. (2021). Effect of iron tailings and slag powders on workability and mechanical properties of concrete. *Frontiers in Materials*, *8*, 723119. https://doi.org/10.3389/fmats.2021.723119

Tao, L. I., & Dang, B. (2016). Experimental study on the compressive strength of iron tailings concrete with different replacement types. *Hebei Journal of Industrial Science and Technology*, *33*, 240–245.

Tayeh, B. A., & Al Saffar, D. M. (2018). Utilization of waste iron powder as fine aggregate in cement mortar. *Journal of Engineering Research and Technology*, *5*(2), 22–27.

Thakur, A., Singh, D., & Singh, A. (2019). Enhancement in properties of cement mortar by using iron-based material: a critical review. *International Journal for Research in Applied Science & Engineering Technology*, *7*(12), 689–691.

Summary

The influence of iron powder content on the fresh and hardened properties of mortar. The growing global waste problem, combined with the environmental impact of concrete production, necessitates innovative solutions to mitigate pollution, conserve resources, and enhance concrete performance. This research explores the potential of iron powder (IP) as a partial cement replacement in mortar. The study investigates the influence of iron powder on the fresh and hardened properties of mortar at seven replacement percentages: 1%, 2%, 3%, 4%, 5%, 10%, and 20% by weight. A comprehensive range of tests, including setting times, air content, density, flow time, compressive strength, and flexural strength, were conducted to assess the performance of the IP-modified mortars. The incorporation of iron powder into mortar mixtures significantly affected its properties. For replacement percentages greater than 3%, a slight enhancement in workability (3%) was observed. In terms of compressive strength, optimal performance was achieved with a 5% iron powder replacement (MIP5), surpassing that of the control mortar despite an increase in air content. Further increasing the iron powder content beyond 5% resulted in a modest decrease in compressive and flexural strengths, confirming that 5% is the optimal replacement percentage. This research provides significant practical implications, offering a viable and sustainable pathway for utilizing industrial waste, reducing landfill burden, conserving natural resources, and developing greener, high-performance construction materials.